
Since January 2020 Elsevier has created a COVID-19 resource centre with free information in English and Mandarin on the novel coronavirus COVID-19. The COVID-19 resource centre is hosted on Elsevier Connect, the company's public news and information website.

# Viral presence and immunopathology in patients with lethal COVID-19: a prospective autopsy cohort study

*Bernadette Schurink*, Eva Roos*, Teodora Radonic, Ellis Barbe, Catherine S C Bouman, Hans H de Boer, Godelieve J de Bree, Esther B Bulle, Eleonora M Aronica, Sandrine Florquin, Judith Fronczek, Leo M A Heunks, Menno D de Jong, Lihui Guo, Romy du Long, Rene Lutter, Pam C G Molenaar, E Andra Neefjes-Borst, Hans W M Niessen, Carel J M van Noesel, Joris J T H Roelofs, Eric J Snijder, Eline C Soer, Joanne Verheij, Alexander P J Vlaar, Wim Vos, Nicole N van der Wel, Allard C van der Wal, Paul van der Valk†, Marianna Bugiani†*

## Summary

**Background** Severe acute respiratory syndrome coronavirus 2 (SARS-CoV-2) targets multiple organs and causes severe coagulopathy. Histopathological organ changes might not only be attributable to a direct virus-induced effect, but also the immune response. The aims of this study were to assess the duration of viral presence, identify the extent of inflammatory response, and investigate the underlying cause of coagulopathy.

**Methods** This prospective autopsy cohort study was done at Amsterdam University Medical Centers (UMC), the Netherlands. With informed consent from relatives, full body autopsy was done on 21 patients with COVID-19 for whom autopsy was requested between March 9 and May 18, 2020. In addition to histopathological evaluation of organ damage, the presence of SARS-CoV-2 nucleocapsid protein and the composition of the immune infiltrate and thrombi were assessed, and all were linked to disease course.

**Findings** Our cohort (n=21) included 16 (76%) men, and median age was 68 years (range 41–78). Median disease course (time from onset of symptoms to death) was 22 days (range 5–44 days). In 11 patients tested for SARS-CoV-2 tropism, SARS-CoV-2 infected cells were present in multiple organs, most abundantly in the lungs, but presence in the lungs became sporadic with increased disease course. Other SARS-CoV-2-positive organs included the upper respiratory tract, heart, kidneys, and gastrointestinal tract. In histological analyses of organs (sampled from nine to 21 patients per organ), an extensive inflammatory response was present in the lungs, heart, liver, kidneys, and brain. In the brain, extensive inflammation was seen in the olfactory bulbs and medulla oblongata. Thrombi and neutrophilic plugs were present in the lungs, heart, kidneys, liver, spleen, and brain and were most frequently observed late in the disease course (15 patients with thrombi, median disease course 22 days [5–44]; ten patients with neutrophilic plugs, 21 days [5–44]). Neutrophilic plugs were observed in two forms: solely composed of neutrophils with neutrophil extracellular traps (NETs), or as aggregates of NETs and platelets..

**Interpretation** In patients with lethal COVID-19, an extensive systemic inflammatory response was present, with a continued presence of neutrophils and NETs. However, SARS-CoV-2-infected cells were only sporadically present at late stages of COVID-19. This suggests a maladaptive immune response and substantiates the evidence for immunomodulation as a target in the treatment of severe COVID-19.

**Funding** Amsterdam UMC Corona Research Fund.



## Introduction

Since the first identification of severe acute respiratory syndrome coronavirus 2 (SARS-CoV-2) in December, 2019, in China, the virus has spread rapidly throughout the globe, causing severe morbidity and mortality from COVID-19.

Analogous to severe acute respiratory syndrome (SARS), the lungs are the first and most severely affected organ by SARS-CoV-2. Histological examinations show T-cell infiltration and subsequent diffuse alveolar damage, presence of thrombi and microthrombi, epithelial multinucleated giant cells, and severe endothelial injury.[1–9] However, as can be expected from the various clinical presentations in patients, the lungs are not the only affected organ. SARS-CoV-2 also targets the heart, kidneys, and intestine.[1,4,5,10,11] Histopathological changes might not only result from a direct virus-induced effect, but also from immune-related changes.[12] Generalised coagulopathy is also seen,[5] causing important morbidity and even mortality.

Although the disease mechanisms are slowly being resolved, clinicians and researchers are only beginning to understand the pathophysiology of COVID-19. Many important questions regarding the disease course and associated coagulopathy remain unanswered. Therefore, the aim of this study was to contextualise histological changes in patients who had died with COVID-19. We evaluated disease course, the presence of virus-infected cells, and the magnitude of the immune response in

*Lancet Microbe* 2020; 1: e290–99

Published Online September 25, 2020 https://doi.org/10.1016/S2666-5247(20)30144-0

*Contributed equally

†Contributed equally

**Department of Pathology** (B Schurink PhD, E Roos PhD, T Radonic PhD, E Barbe PhD, E A Neefjes-Borst MD, Prof H W M Niessen PhD, W Vos MSc, Prof P van der Valk PhD, M Bugiani PhD), **Department of Intensive Care Medicine** (Prof L M A Heunks PhD), **and Department of Cardiac Surgery, Amsterdam Cardiovascular Sciences** (Prof H W M Niessen), **Amsterdam University Medical Centers (UMC), VU University Amsterdam, Amsterdam, Netherlands; Department of Intensive Care Medicine** (C S C Bouman PhD, E B Bulle MD, A P J Vlaar PhD), **Department of Pathology** (H H de Boer PhD, Prof E M Aronica PhD, Prof S Florquin PhD, J Fronczek PhD, R du Long MD, Prof C J M van Noesel PhD, J J T H Roelofs PhD, E C Soer PhD, J Verheij PhD, Prof A C van der Wal PhD), **Department of Medical Microbiology** (Prof M D de Jong PhD), **Department of Pulmonary Diseases** (R Lutter PhD, P C G Molenaar BSc), **and Electron Microscopy Center Amsterdam, Department of Medical Biology** (N N van der Wel PhD), **Amsterdam UMC, University of Amsterdam, Amsterdam, Netherlands; Department of Forensic Medicine, Netherlands Forensic Institute, The Hague, Netherlands** (H H de Boer, J Fronczek); **Department of Internal Medicine** (G J de Bree PhD) **and Department of Experimental Immunology** (L Guo PhD,

R Lutter), **Amsterdam Infection and Immunity Institute, Amsterdam UMC, University of Amsterdam, Amsterdam, Netherlands; and Molecular Virology Laboratory, Department of Medical Microbiology, Leiden University Medical Center, Leiden, Netherlands** (Prof E J Snijder PhD)

Correspondence to: Dr Marianna Bugiani, Department of Pathology, Amsterdam UMC, VU University Amsterdam, 1081 HV Amsterdam, Netherlands **m.bugiani@amsterdamumc.nl**

## Research in context

### Evidence before this study

At the start of this study in March, 2020, insight was limited into the extent of organ involvement in COVID-19. Reported autopsy findings mainly described pulmonary disease with diffuse alveolar damage in a few cases. This was later confirmed in an autopsy study of the lungs that described endotheliitis and thrombosis in patients with COVID-19. Involvement of other organs has been suggested in patients with systemic and severe progressive disease who have cardiac, neurological, and gastrointestinal symptoms. Severe acute respiratory syndrome coronavirus 2 (SARS-CoV-2) has been shown to infect the kidneys and cause damage to the glomeruli. Hypoxic changes have been described in the brain, and neurological symptoms are frequently observed in patients with COVID-19. Observed thromboembolic events have been suggested to be caused by an effect of the virus on the vascular walls, but whether coagulopathy was systemic remained unknown. We aimed to assess the duration of viral presence, identify the extent of the inflammatory response, and investigate the nature of the coagulopathy.

### Added value of this study

In patients with lethal COVID-19, organs were mainly affected by an inflammatory response. Extensive inflammatory changes in the brain, especially in the olfactory bulbs and medulla oblongata, might cause anosmia and dampening of the respiratory system. Sporadic SARS-CoV-2 infected cells were present up to 6 weeks after the onset of symptoms. A continuous presence of neutrophils with formation of neutrophil extracellular traps (NETs) was seen in the lungs, heart, kidneys, liver, and brain. Disproportionate presence of inflammation with aggregated neutrophils and NETs in comparison with the sporadic presence of virus suggests an autonomous maladaptive immune response. Neutrophils and NETs frequently formed aggregates with platelets, suggesting a role in the poorly understood systemic coagulopathy.

### Implications of all the available evidence

Generalised sustained activation of the innate immune system with formation of NETs encapsulating thrombi and platelets, in combination with sporadic presence of SARS-CoV-2-infected cells, suggests an autonomous maladaptive immune response is the primary driver of lethal COVID-19. NETs seem to have a role in the maintenance of coagulopathy in patients with COVID-19. This study underlines the importance of targeting the immune response in patients with COVID-19 and substantiates the possible beneficial effects of low-dose dexamethasone in the treatment of COVID-19. Our findings generate novel questions surrounding the potential role of NETs in persistent immune activation and in SARS-CoV-2-induced coagulopathy.

various affected organs. In addition, the composition of thrombi was assessed to elucidate the underlying cause of the coagulopathy. These important questions need to be resolved to optimise treatment for critically ill patients with COVID-19.

## Methods

### Study design and participants

This prospective autopsy cohort study was done at Amsterdam University Medical Centers (UMC), the Netherlands, at the VU Medical Center and Academic Medical Center. Ethical approval was granted by the institutional review board of Amsterdam UMC.

21 patients with clinically confirmed COVID-19 for whom autopsy was requested between March 9 and May 18, 2020, were included. COVID-19 was confirmed during hospital admission by quantitative real-time RT-PCR. Informed consent for complete autopsy (with additional consent for the brain) was obtained from the decedents' next of kin.

### Procedures

See Online for appendix

During autopsy all organ systems were extensively sampled (appendix p 2). Sampling included the lungs, upper respiratory tract, submandibular gland, heart, gastrointestinal tract, kidneys, adipose tissue, and brain. Samples were formalin fixed, paraffin embedded, sectioned, and stained with haematoxylin and eosin (HE). To characterise HE findings, additional histochemical and immunohistochemical stains were done (appendix p 3). All organ sections were evaluated by at least two dedicated organ specialists. Presence of SARS-CoV-2 was revealed by two different antibodies against the SARS-CoV-2 nucleocapsid protein: a non-commercial monoclonal mouse antibody[13] and a polyclonal rabbit antibody[14] (Sino Biological and Nanommune, Irvine, CA, USA). Positive staining was defined as cytoplasmic staining of the same cell type by both antibodies. In cases of discordant staining of the antibodies, the result was considered negative. Optimisation steps for the SARS-CoV-2 staining protocol are detailed in the appendix (p 4). Quantitative real-time RT-PCR was done on lung samples of this subset (appendix p 4). However, because RT-PCR results were possibly negatively influenced by post-mortem tissue quality and were often deemed of too low quality, they are not elaborated on in this paper. Density of the SARS-CoV-2 infiltrate was described as percentage of immunopositive cells per high-power field, and arbitrarily defined as sporadic (1–5%), moderate (>5% to 10%), and dense (>10%). The innate and adaptive immune response were characterised by staining for myeloperoxidase (MPO) and citrullinated histone 3 (citH3; as a marker of neutrophil extracellular traps [NETs]), and CD4, CD8, and CD20. Additional granzyme B, HLA-DR, myelin basic protein,

and glial fibrillary acidic protein (GFAP) stains were done on brain tissue. The presence and composition of thrombi were assessed with CD61, Periodic acid–Schiff, fibrin, complement component C3d, MPO, and citH3 stains. Antibody details for all aforementioned markers are provided in the appendix (pp 3–4). The immunohistochemical analyses of brain tissue and SARS-CoV-2 distribution were only available for samples at one location (n=11) due to logistical issues during the pandemic. Baseline characteristics were not significantly different between locations (appendix p 5).

### Clinical data collection and data analysis

Clinical data were extracted from electronic patient files and stored in Castor Electronic Data Capture. Descriptive statistical analyses were done with SPSS (version 24.0). Variables were presented as the median and range on the basis of the small number of included patients. Proportions were compared with the $\chi^2$ test and medians were compared with the Mann-Whitney *U* test. Because this was an unpowered observational cohort study, significance (p value <0·05) is only displayed in the appendix.

The clinical and histological definitions used in assessments of patients and samples are provided in the appendix (p 6).

### Role of the funding source

The funder of the study had no role in study design, data collection, data analysis, data interpretation, or writing of the report. ER, BS, MB and PvdV had full access to all the data in the study. The corresponding author had final responsibility for the decision to submit for publication.

## Results

In our cohort of 21 patients, most were men (16 [76%] of 21), and median age was 68 years (range 41–78). Median disease course (days between onset of symptoms and death) was 22 days (range 5–44 days). Most patients (16 [76%]) were admitted to the intensive care unit. Of the total cohort, nine (43%) patients died of COVID-19 pneumonia with respiratory failure, and seven (33%) of multiorgan failure. The remaining five patients died from other causes: pulmonary embolism (two [10%] patients), haemorrhagic stroke (one [5%]), surgical complication leading to bacterial peritonitis (one [5%]), and a neurological condition of unknown cause (necrotising encephalitis, potentially developing before COVID-19; one [5%]). The short durations of disease in our cohort (minimum 5 days) enabled us to study disease in a relatively early phase. Median time from death to autopsy was 15 h (range 3–88). Baseline characteristics of patients are shown in the table.

Presence of SARS-CoV-2 was evaluated in 11 patients (appendix p 7). In all patients, SARS-CoV-2 immunohistochemistry was positive in at least one organ. In eight (73%) patients, SARS-CoV-2 infection was identified in the lungs in type 1 and type 2 pneumocytes, endothelial cells, bronchial epithelium, and intra-alveolar macrophages. Median disease course in these patients was 14 days (range 5–31). The presence of infected cells varied between sporadic (1–5% of total cells per high-power field), moderate (>5% to 10%), and dense (>10%) in patients with a short disease course (median 7 days [5–10]; n=4), whereas infected cells were only sporadically present in patients with a longer disease course (median 23 days [17–31]; n=4; figure 1). The median disease course of patients with negative lung staining was 27 days (12–44; n=3); in these patients, SARS-CoV-2-infected cells were sporadically to moderately present in other organs.

In subsets of patients, sporadic SARS-CoV-2-positive cells were present in the major airways (trachea, bronchi, and bronchioles; two [18%] of 11 patients), submandibular glands (three [27%] patients), and crypts of the duodenum and endothelium of the stomach and ileum (three [27%] patients; figure 1). The median disease course in these patients was 20 days (range 8–31), 12 days (8–17), and 8 days (5–10), respectively. Cardiomyocytes (in three [27%] patients), liver vascular endothelium (two [18%] patients), and tubular epithelium of the kidney (one [9%] patient; figure 1) also contained SARS-CoV-2-infected cells in sporadic or moderate abundance (median disease courses of 10 days [6–44], 11 days [5–17], and 8 days, respectively). Of the patients with systemic presence, six had positive lung staining and two had negative lung staining. SARS-CoV-2 immunohistochemistry was sporadically positive in cells in the mesocolic fat (in one [9%] patient), and omental fat and pancreas (two [18%] patients), with median disease courses of 24 days, 17 days (range 10–24), and 17 days (range 10–24), respectively (figure 1). Positive macrophages were seen in the bone marrow of one (9%) patient (disease course 27 days; figure 1) and in the spleen of another patient (disease course 24 days; images not shown). Immunohistochemistry was negative in the skeletal muscle, genital tract, and brain.

Three of 21 patients were excluded from lung histology analysis due to lack of extensive lung sampling (no sample of the peripheral and central parenchyma of each lobe). In all analysed patients, various patterns of diffuse alveolar damage were present. We observed an exudative pattern in 14 (78%) of 18 patients, a proliferative pattern in 15 (83%) patients, and a fibrotic pattern in four (22%) patients (figure 2). Bronchopneumonia was found in seven (39%) patients, of whom one had an *Aspergillus* superinfection confirmed by PCR. A patchy distribution of histopathological patterns was seen with severely and sparsely affected areas in close proximity (figure 2). In each patient, a predominant pattern was identified, of either exudative diffuse alveolar damage (three [17%] patients), bronchopneumonia (three [17%] patients), or proliferative diffuse alveolar damage (12 [67%] patients). In four patients, of whom one had mainly bronchopneumonia and three had mainly a proliferative pattern, initial signs of fibrosis were observed. Of 14 patients who died due to

| | Total (n=21) |
|---|---|
| Age, years | 68 (41–78) |
| Sex | |
| Male | 16 (76%) |
| Female | 5 (24%) |
| Comorbidity | 16 |
| Diabetes | 1 (7%) |
| Cardiovascular disease | 6 (38%) |
| Chronic obstructive pulmonary disease | 2 (13%) |
| Asthma | 0 |
| Active solid malignancy | 1 (7%) |
| Active haematological malignancy | 2 (13%) |
| Other* | 4 (25%) |
| Intoxications† | |
| Yes | 3 (14%) |
| No | 8 (38%) |
| Missing | 10 (48%) |
| Body-mass index, kg/m² | 27 (26–32) |
| Hospital characteristics | |
| Hospital admittance‡ | 21 (100%) |
| Time between first symptoms and hospital admittance, days | 8 (5–14) |
| ICU admittance | 16 (76%) |
| Duration in ICU, days | 12 (8–20) |
| Invasive mechanical ventilation | 16 |
| Vasopressors | 16 |
| Continuous renal replacement therapy | 5 |
| Medication during admittance | 21 (100%) |
| Antibiotics | 20 (95%) |
| Chloroquine | 10 (48%) |
| Antiviral drugs | 4 (19%) |
| Antifungal | 9 (43%) |
| Steroids (high-dose)§ | 5 (24%) |
| Other disease manifestations | |
| Thromboembolic events | 10 (48%) |
| Deep venous thrombosis | 3 |
| Pulmonary embolism (thrombosis) | 6 |
| Both | 1 |
| Cardiac events | 13 (62%) |
| Arrhythmias | 12 |
| Ischaemic events | 0 |
| Heart failure | 1 |
| (Continued from previous column) | |
| Renal failure¶ | 15 (71%) |
| KDIGO stage 1 | 2 |
| KDIGO stage 2 | 3 |
| KDIGO stage 3 | 10 |
| Neurological events | 10 (48%) |
| Delirium | 5 |
| Cerebrovascular accident (acute stroke) | 2 |
| Other‖ | 3 |
| Necrotising encephalitis | 1 |
| Hypoxic encephalopathy | 2 |
| Suprainfection (%) | 9 (43%) |
| Aspergillus** | 8 |
| Bacterial | 1 |
| Viral | 0 |
| Autopsy characteristics | |
| Disease course from symptom onset, days | 22 (5–44) |
| Time from death to autopsy, h | 15 (3–88) |
| Autopsy diagnosis cause of death | |
| COVID-19 pneumonia | 9 (43%) |
| Pulmonary embolism | 2 (10%) |
| Cerebrovascular accident (acute stroke) | 1 (5%) |
| Multiorgan failure | 7 (33%) |
| Other†† | 2 (10%) |

Data are median (range), number of patients (%), or number of patients. ICU=intensive care unit. KDIGO=Kidney Disease: Improving Global Outcomes. *All neurological including one patient with Alzheimer's disease. †Intoxications in three patients were the use of tobacco or alcohol at the time of admittance; information only available in nine of 21 patients. ‡One male patient died a day after discharge from a conventional ward after admittance for COVID-19. §High-dose steroids were defined as more than 10 mg prednisone or more than 40 mg hydrocortisone per day according to local definitions. ¶Renal failure was defined according to the 2012 KDIGO guideline for acute kidney injury.[35] ‖Brain autopsy was done in the patient with necrotising encephalitis. **Other fungal infections were not found. ††One patient died due to necrotising encephalitis and one due to bacterial peritonitis after abdominal surgery for solid malignancy (placement of gastrojejunostomy) with a subsequent anastomotic leak.

***Table:*** **Baseline characteristics**

COVID-19-related causes, 11 (79%) had primarily proliferative diffuse alveolar damage. Patients with a predominantly proliferative pattern had a median disease course of 25 days (range 12–44; n=12).

All patients had T-cell infiltrate in the interstitial space; this was CD4-mediated in patients with exudative diffuse alveolar damage and bronchopneumonia, and CD8-mediated in patients with proliferative diffuse alveolar damage (images not shown). Neutrophils in the interstitial spaces and neutrophilic plugs in the capillaries were seen in all patients. Endotheliitis and microthrombi (≤100 µm) were present in 15 (83%) patients, seven of whom also had macrothrombi (>100 µm; figure 2). Pulmonary megakaryocytes were abundantly present in these patients. Areas of necrosis were found in three (17%) patients. These histological findings were independent of diffuse alveolar damage pattern and also present in unaffected areas (figure 2).

Other organs were frequently affected by congestion, consistent with prolonged haemodynamic instability and intensive care treatment. Detailed descriptions of tissue histology are provided in the appendix (pp 8–9). In the heart, inflammatory infiltrates were found in either the endocardium, myocardium, epicardial fat, or in combinations of these tissues, sometimes associated with fibrosis, suggesting an early onset of manifestations

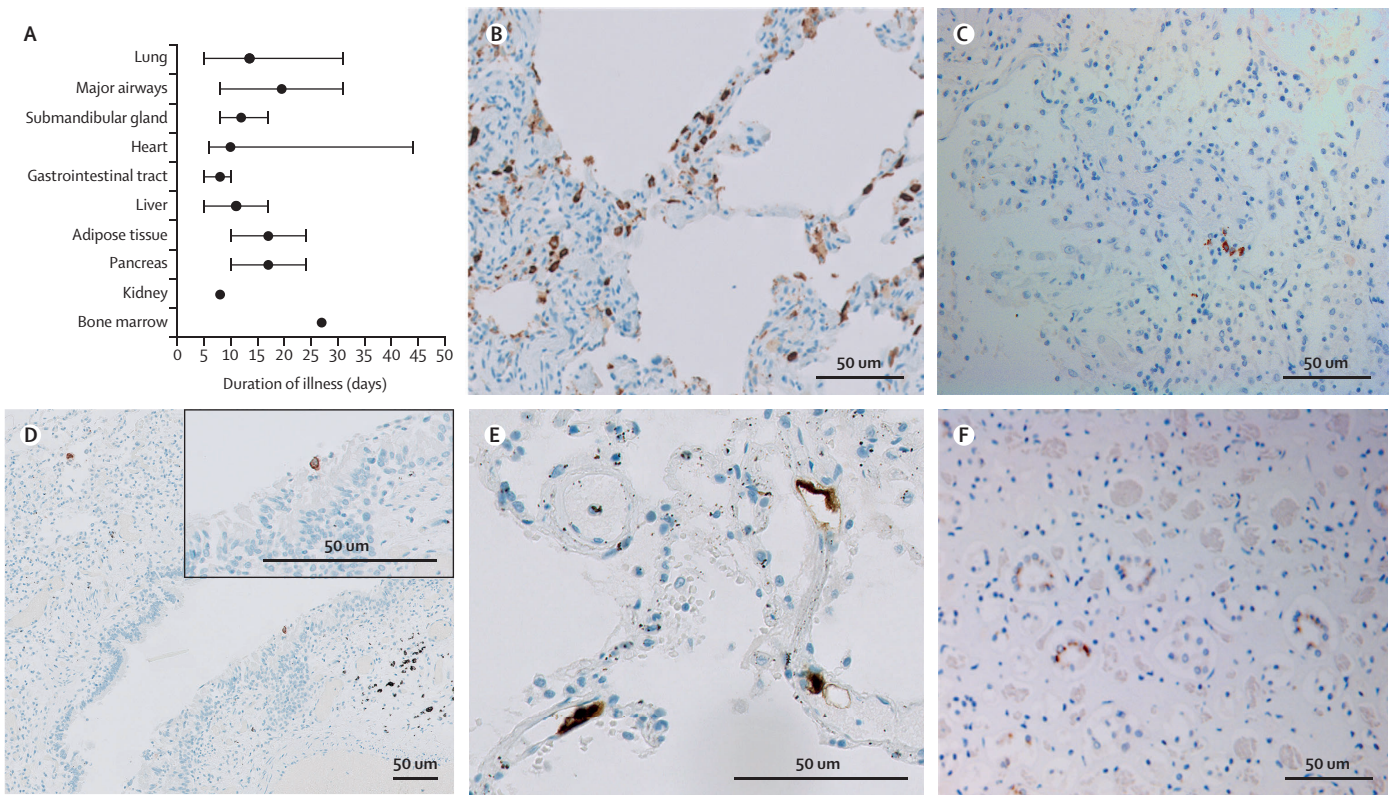


***Figure 1:*** **SARS-CoV-2 tropism**

Two antibodies against SARS-CoV-2 nucleocapsid protein were used to detect infected cells. Staining of the same cell type by both antibodies was considered as positive immunoreactivity. (A) Median disease course per organ group with immunoreactivity for SARS-CoV-2. Error bars indicate the range. Adipose tissue consisted of mesocolic fat or omental fat (or both). The appendix (p 7) shows SARS-CoV-2 positivity per organ per patient. (B) Stain against SARS-CoV-2 in the lung of a patient with mainly exudative diffuse alveolar damage and a disease course of 5 days. Immunoreactive cells were abundant (>10% infected cells per high-power field). Infected cells were pneumocytes along the alveolar walls, stromal cells in the septae, endothelial cells in the small blood vessels, and alveolar macrophages. (C) Stain against SARS-CoV-2 in the lung later in the disease course (patient with a disease course of 22 days) revealed only scattered immunoreactive cells, conceivably pneumocytes. (D) Stain against SARS-CoV-2 in the lung later in the disease course (patient with a disease course of 31 days) also showed immunopositivity in a respiratory cell lining a bronchiole. (E) Stain against SARS-CoV-2 in the lung early in the disease course (patient with a disease course of 5 days [also represented in part B]) showed immunopositive endothelial cells in septal capillaries. (F) Stain against SARS-CoV-2 in the kidney (patient with a disease course of 24 days) revealed immunoreactivity of the distal tubular epithelial cells. SARS-CoV-2=severe acute respiratory syndrome coronavirus 2.

(appendix pp 8, 10). Epicardial and endocardial lymphohistiocytic infiltration (positive for CD68 and CD45) was found in all patients analysed for cardiac changes (n=20 with complete atria and ventricle sampling). Inflammatory changes in the myocardium, characterised by presence of histiocytes, T cells (CD3-positive), and neutrophils, were found in 11 (55%) patients. Myocyte injury was observed in the left ventricle in all 20 (100%) patients and in the right ventricle in 12 (60%) patients (appendix p 8). Accompanying fibrin platelet thrombi were present in the small intramyocardial blood vessels in 11 (47%) patients, and in the endocardial mural blood vessels in three (15%) patients (appendix p 8).

Among all 21 patients, renal histopathological changes were found in 12 (57%) patients (median disease course 16 days [range 5–44]), consisting of tubular dilation, simplification of tubular epithelial cells, and loss of the tubular epithelial cell brush borders, most prominent in the corticomedullary transition zones (appendix pp 8–9, 11). These 12 patients also showed tubular epithelial cell vacuolisation in the proximal tubules. Glomerular microthrombi (positive for fibrin and CD61) were present in one (5%) patient (appendix pp 8–9, 11). Three (14%) patients (median disease course 31 days [5–44]) showed neutrophilic aggregates in blood vessels, mixed with platelets (as observed on HE and CD61 staining; appendix p 9). One (5%) patient showed signs of endothelial activation, characterised by mild endothelial swelling and arteriolar sequestration of leucocytes on HE staining (images not shown). No specific glomerular cell changes were evident, apart from pre-existent glomerular sclerosis or signs of glomerular ischaemia. Pre-existent chronic tissue damage, partly related to ageing, was seen in ten of the 21 patients.

Brain autopsy was consented for in nine patients (figure 3). Brain hypoxic changes, manifesting as hypereosinophilia or nuclear and cytoplasmatic condensation of neurons in the cerebrum and cerebellum on HE staining, were observed in all patients, of whom five were mechanically ventilated. All patients showed an extensive inflammatory response, affecting both white and grey

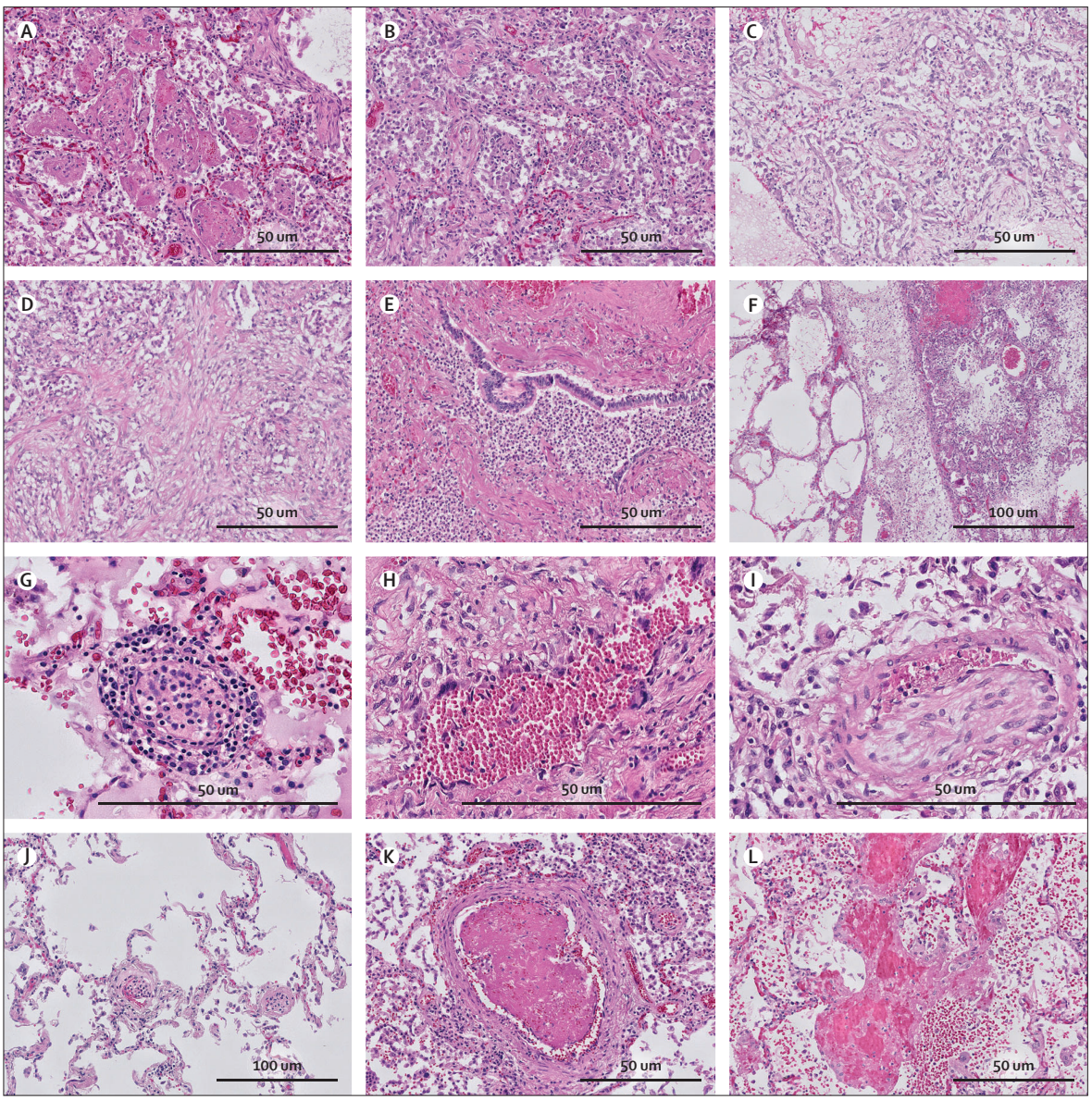


***Figure 2:*** **Lung histopathology in COVID-19**
Different phases of diffuse alveolar damage were identified in COVID-19 (haematoxylin and eosin stain). (A) Exudative pattern with intra-alveolar fibrin exudation. (B) Exudative pattern with desquamation with early fibroblastic proliferation. (C) Proliferative diffuse alveolar damage with fibroblastic proliferation in the alveoli, partially incorporated in the alveolar septa. (D) Fibrosing phase of alveolar damage with collagen deposition (pink) in the areas with fibroblastic proliferation. (E) Exudative bronchopneumonia with neutrophil granulocyte infiltration of bronchi and surrounding alveolar parenchyma. (F) Patchy distribution of the acute damage and prominent lymphatic stasis in the septa. (G) Endotheliitis of small vessels (<100 µm) with infiltration of the endothelium and vessel wall by lymphocytes and plasma cells. (H) Giant cell transformation of the endothelium in a patient with longstanding COVID-19 (disease course 30 days). (I) Chronic thromboembolic vasculopathy with an organised thrombus in an arteriole. (J) Patchy thrombi in microvessels (<70 µm) and segregation of thrombocytes and neutrophil granulocytes in the vessels in the spared lung parenchyma. (K) New-formed thrombus in an arteriole. (L) Focal necrosis of the alveolar septa with blood and fibrin exudation in the parenchyma.

matter, irrespective of disease course (median 11 days [range 5–31]). The response was present in all regions examined (figure 3) and most severe in the cranial medulla oblongata and olfactory bulb, characterised in all nine patients by activation and clustering of microglia (HLA-DR-positive), astrogliosis (GFAP-positive), and perivascular cuffing of T cells (CD3-positive). Sparse T cells (CD3-positive, and CD4-positive, or CD8-positive) were also noted in the parenchyma in all patients. Neutrophilic plugs were identified in three (33%) patients, with a disease course of 8, 22, and 25 days (appendix pp 9, 11). No loss of myelin or haemorrhages were seen (figure 3).

Bone marrow was analysed in 15 patients with sufficient sampling. Trilinear hyperplasia of haematopoietic cell lineages in the bone marrow was observed in ten (67%) patients. Bone marrow showed discrete fibrosis and

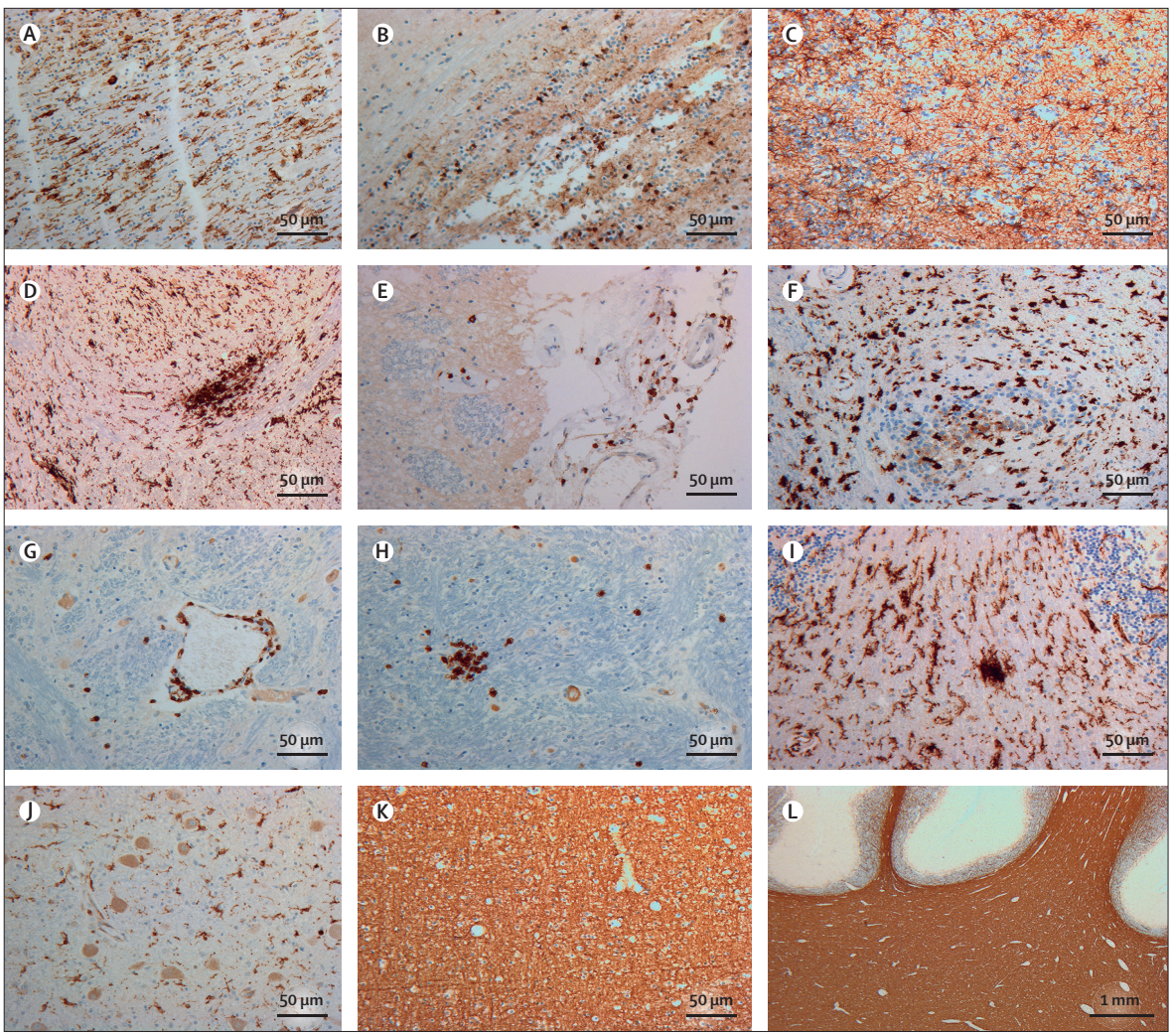


***Figure 3:*** **Neuroinflammatory response to COVID-19 in the brain**
(A) Stain against HLA-DR in the bulbus olfactorius showed numerous activated microglia with enlarged cell bodies and thick cell processes longitudinally arranged. (B) Stain against CD3 in the bulbus olfactorius revealed T-cell extravasion into the parenchyma. (C) Stain against glial fibrillary acidic protein in the bulbus olfactorius showed reactive astrocytes in an anisomorphic arrangement. (D) Stain against HLA-DR in the medulla oblongata in the region of the nucleus of the tractus solitarius showed massive microglia activation with formation of a large cell aggregate (microglia nodule). (E) Stain against CD3 in the dorsal aspect of the medulla oblongata revealed T cells in the leptomeninges. (F) Stain against HLA-DR in the cervical spinal cord showed activated microglia with ameboid morphology also in this region. (G) Stain against CD3 in the medulla oblongata indicated a perivascular cuffing of T cells; some cells can also be seen in the surrounding parenchyma. (H) Stain against CD3 in the medulla oblongata confirmed presence of intraparenchymal T cells, aggregated in small nodules. (I) Stain against HLA-DR in the cerebellum showed numerous activated microglia with enlarged cell bodies and thick processes in the white matter of the basis of a folium; a small microglia nodule was also present. (J) Stain against HLA-DR of the nucleus dentatus revealed activated microglia also in the cerebellar structures of deep grey matter. (K) Stain against the major myelin protein, MBP in the frontal lobe revealed preservation of myelin in the cerebral white matter. (L) Stain against MBP in the cerebellum showed intact myelin in the deep hemispheric regions and the folia. MBP=myelin basic protein.

abnormalities in megakaryocytes, with increased megakaryocyte numbers (12 [80%] patients), clustering (four [27%] patients), and abnormal morphology of these cells (11 [73%] patients; appendix pp 8, 11).

Overall, thrombi were detected in 15 patients and neutrophilic plugs in ten patients by HE, MPO, and citH3 staining (figures 2, 4, appendix pp 9–11). NET formation was observed and exemplified by swollen nuclei positive for citH3 staining (figure 4). Patients with thrombi had a median disease course of 22 days (range 5–44) and those with neutrophilic plugs had a median disease course of 21 days (5–44). Thrombi consisted of fibrin, platelets (positive for CD31 and CD61), and neutrophils in various combinations. Neutrophilic plugs were composed of aggregates of NETs and platelets, or single neutrophils with NET formation without the presence of platelets. These aggregates were seen systemically, localised in the lung, heart, liver, and brain (figure 4, appendix p 9). In the intracerebral vasculature, plugs consisted of aggregated neutrophils without apparent formation of NETs

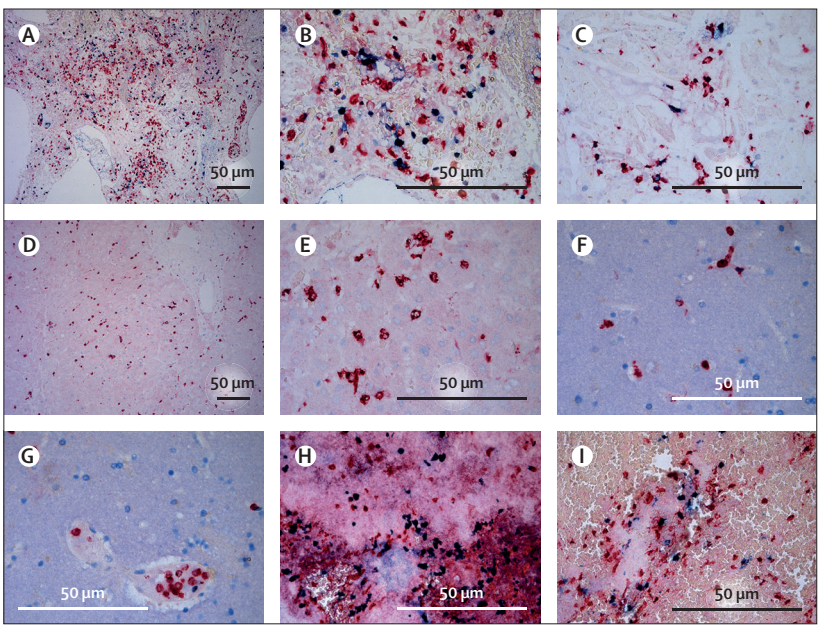


***Figure 4:*** **Presence of neutrophils and formation of neutrophil extracellular traps**
Tissue sections of patients who died of severe acute respiratory syndrome coronavirus 2 infection were stained for myeloperoxidase (red), as a marker of neutrophilic granulocytes, and citrullinated histone 3 (blue), as a marker of extracellular DNA traps and where extracellular co-localisation suggests trap formation by neutrophils. (A and B) Lung tissue showed abundant presence of neutrophils in both the lung vasculature and parenchyma with formation of neutrophil extracellular traps in a patient with a disease course of 8 days. (C) Heart tissue showed the presence of neutrophils in and surrounding cardiac vessels and in the cardiac parenchyma with formation of neutrophil extracellular traps in a patient with a disease course of 17 days. (D and E) Liver tissue showed the presence of neutrophils in the liver parenchyma but no extracellular traps in a patient with a disease course of 27 days. (F and G) Brain tissue showed the presence of neutrophils within the cerebral vasculature but no extracellular traps in a patient with a disease course of 8 days. (H and I) Thrombus in the main bronchus showed abundant presence of neutrophils with formation of neutrophil extracellular traps in a patient with a disease course of 8 days.

(appendix p 11). Only one patient with neutrophilic plugs had sporadically infected SARS-CoV-2 cells in the same organ (liver).

## Discussion

Our results show that COVID-19 is a systemic disease. Almost all organs harbour SARS-CoV-2 immune-positive cells, detectable up to 6 weeks after onset of symptoms. In the lungs, SARS-CoV-2 was present in the greatest abundance, mainly early in the disease course. Inflammatory changes most frequently occurred in the lungs, heart, kidneys, and brain. In the brain, extensive inflammation was detected, which was most pronounced in the olfactory bulbs and medulla oblongata.

Evaluation of the immune infiltrate showed notable presence of aggregated neutrophils in all patients in the lungs and several other organs, even after a disease course of several weeks. Neutrophilic plugs with NET formation were present in the heart, kidney, liver, and brain, admixed with platelets in some cases. This finding suggests involvement of NETs in coagulopathy and prolonged activation of neutrophils in lethal COVID-19, or at least a delayed resolution of these NETs.

Limitations of this study should be considered. A major difficulty in tissue histology is the correlation between histopathological findings and the clinical substrate. In our cohort, extensive intensive care treatment, medication, and direct cytopathic effects would have been intertwined and provided multiple mechanisms resulting in damage on a cellular level, challenging the interpretation of results. A control cohort with, for example, patients with lethal influenza, would be of value to provide perspective to our histopathological findings. Inherent to autopsy studies, our results are biased towards severe pathology. However, patients with short symptomatology and other causes of death were included, representing earlier stages of COVID-19. Whether findings in these patients represent a less severe form of COVID-19 cannot be determined. Immunohistochemistry was used to illustrate viral presence in specific cell types. Although immunohistochemistry has the possibility to elucidate the affected cell type, RT-PCR in general is more specific for determining viral presence. However, post-mortem decay affects RNA quality (appendix p 4).[16,17] To increase the validity of our findings, immunohistochemistry for SARS-CoV-2 was done with two antibodies that have been verified in SARS-CoV2-infected cell lines and influenza-infected tissue to ensure reliability.[13,14]

The results of this study confirm that COVID-19 causes diffuse alveolar damage in the lungs.[1,2,4–7,18–20] Different patterns of diffuse alveolar damage were present simultaneously, sometimes in combination with endotheliitis, and macrothrombi and microthrombi. In patients who died due to COVID-19, the proliferative pattern, associated with low diffusion and ventilation capacity, was predominant. Diffuse alveolar damage is a condition that is seen in other viral infections including SARS, Middle East respiratory syndrome, and several types of influenza.[21–23] Analogous to other cohorts of patients with COVID-19,[10,18,19,24–27] inflammatory changes in the heart, kidney, and brain were also present. Mild hepatic portal inflammation was also present in more than half of patients, which might represent a mainly immune mediated or toxic effect, given that viral presence would probably cause a heavier infiltrate. In the kidney, tubular epithelial cell vacuolisation was frequently seen. This event, in contrast to acute tubular necrosis, is uncommon in autopsy cases. With immunohistochemistry, SARS-CoV-2-positive cells were present in the tubular epithelium in one patient. It could be speculated that tubular epithelial cell vacuolisation is directly attributable to viral presence in the tubular epithelium. However, the vacuolisation could also represent a toxic effect of medication.[24,28]

In the heart, inflammatory changes with lymphohistiocytic infiltration were observed. These histological patterns have low specificity for the type of myocyte injury. They could relate to either virally induced inflammation, myocardial stress, ischaemia, drugs, microvascular thrombotic occlusion, or combinations of these factors.[25] In our cohort, not all patients with cardiac inflammation

showed electrocardiogram abnormalities attributable to myocarditis, ischaemia, or cardiac failure, or positive cardiac staining for SARS-CoV-2. The lack of a clear clinical substrate is in line with the findings of Lindner and colleagues[26] and others.[3–5,18,19] Establishing a histopathological correlation remains difficult in severely ill patients with a systemic inflammatory response. However, the findings of Puntmann and colleagues,[29] describing myocyte injury post-COVID-19 on MRI, suggest a clinical substrate for COVID-19-induced cardiac damage.

With regard to cerebral involvement, previous post-mortem studies show hypoxic changes and presence of a lymphocytic infiltrate.[27,30] The severe innate inflammatory state seen in our cohort, involving massive activation of microglia with formation of nodules, has not been described previously, possibly due to the lack of specific staining by others.[27] Immunohistochemically and with RT-PCR, we did not detect presence of SARS-CoV-2 in the brain, in contrast to others who found low concentrations by RT-PCR in subsets of patients (five patients, region not specified,[30] and eight patients, in the medulla, frontal lobes, and olfactory nerve[10]). Such findings could indicate either swift viral clearance or a severe autonomously regulated effect. We hypothesise that a large inflammatory response quickly leads to viral clearance. This idea is substantiated by the presence of T cells, and extensive microglial activation with formation of nodules in a patient who died 5 days after onset of symptoms (due to a surgical complication). The brain tissue of this patient did not contain SARS-CoV-2-infected cells. The inflammatory reaction was most pronounced in the olfactory bulbs, which could be linked to the frequent symptom of anosmia in patients with COVID-19.[31] The medulla oblongata has a role in regulation of the respiratory system and is a centre of respiratory rhythm generation.[32] Extensive inflammation of this structure might add to the respiratory failure observed in patients with COVID-19.

A severe immune-mediated response was key in the histopathological changes observed in several organs. SARS-CoV-2-positive cells were most frequently present in the lungs, heart, kidneys, gastrointestinal tract, submandibular glands, and liver at early stages of the disease and only sporadically present in organs in patients with a longer disease course. A swift immune response might decrease the extensive presence of the virus, shifting the pathology towards an autonomous immune-mediated reaction. Notable presence of neutrophils with formation of NETs was seen, even in patients with a long disease course.

Studies over the past decades have established that viral infections, such as influenza and hantavirus, can induce NET formation.[33] In addition to capturing microorganisms, DNA traps have been linked to acute renal damage and thrombosis.[34,35] Although DNA traps can bind bacteria and viruses, we found sporadically present or no SARS-CoV-2-infected cells in patients with abundant neutrophilic aggregates. Therefore, NET formation might not be associated with abundant viral presence. Instead a maladaptive immune stimulation could occur, resulting in continuous neutrophil activation and organ damage. In murine models, processes underlying lethal influenza can be distinguished from non-lethal influenza by a neutrophilic response exaggerated by chemokines,[36] which has been confirmed in patients with influenza.[37]

In SARS-CoV-2, NET formation has been postulated as a predisposing factor to thrombi formation.[38] We validated this hypothesis by showing marked DNA traps and early NET formation (swollen citH3-positive nuclei) in several organs. The frequently observed NETs and NET–platelet aggregates suggest a contribution to the poorly understood coagulopathy in COVID-19. The presence of abnormal megakaryocytes, as seen in the bone marrow, might further add to the coagulopathy by disrupting platelet formation. Virus-induced endotheliitis and aggregation of platelets to the activated vascular wall, evoking the formation of NETs, could be an alternative mechanism for coagulopathy. However, when evaluating our own findings this mechanism does not fully explain the coagulopathy, as thrombi were also present in organs with an unaffected vasculature. Future clinical studies should focus on NET and thrombi formation. Furthermore, the influence of abnormal megakaryocyte formation on platelet function requires investigation.

In conclusion, in patients with lethal COVID-19, organs are mainly affected by an inflammatory response. Extensive inflammatory changes in the brain, especially in the olfactory bulbs and medulla oblongata, might cause anosmia and dampening of the respiratory system. Virally infected cells are sporadically present up to 6 weeks after the start of symptoms, and neutrophils and NETs are present for weeks after onset of symptoms. The formation of NET–platelet aggregates might have a role in COVID-19-associated coagulopathy. The disproportionate presence of aggregated neutrophils and NETs in comparison with the sporadic presence of virus suggests an autonomous maladaptive immune response. This study underlines the importance of targeting the immune response in patients with COVID-19 and substantiates the possible beneficial effects of low-dose dexamethasone in the treatment of COVID-19.[39] The implied role of NETs in persistent immune activation and in SARS-CoV-2-induced coagulopathy has created novel questions in the understanding of COVID-19.

**Contributors**

BS and ER contributed equally to study design, data acquisition, analysis, and interpretation, and drafting and revision of the manuscript. MB and PvdV were the principal investigators and contributed equally to conception and design of the study, acquisition and interpretation of data, and drafting and revision of the manuscript. TR, NNvdW, RL, MDdJ, GJdB, WV, ECS, LG, and ACvdW contributed to the design of the study, development of laboratory methods, acquisition and interpretation of data, and revision of the manuscript. EB, CSCB, HHdB, EMA, EBB, SF, JF, LMAH, PCGM, EAN-B, HWMN, CJMvN, ECS, RdL, JJTHR, EJS, JV, and APJV contributed to acquisition and interpretation of data and revision of the manuscript. All authors agreed to be accountable for all aspects of the work and gave final approval of the manuscript.

**Declaration of interests**
We declare no competing interests.

**Acknowledgments**
We are thankful to the autopsy assistants of the VU Medical Center and Academic Medical Center (Amsterdam University Medical Centers), for their invaluable role during the autopsies. We would like to acknowledge Petra Scholten, Pim Kortman, and Jeannette Pankras for their support in the logistics of this study, all employees of the pathology laboratories of both locations for their work in processing tissue, and Yvonne van der Meer for her revision of the virological data.

**References**

1 Menter T, Haslbauer JD, Nienhold R, et al. Postmortem examination of COVID-19 patients reveals diffuse alveolar damage with severe capillary congestion and variegated findings in lungs and other organs suggesting vascular dysfunction. *Histopathology* 2020; **77:** 198–209.

2 Ackermann M, Verleden SE, Kuehnel M, et al. Pulmonary vascular endothelialitis, thrombosis, and angiogenesis in COVID-19. *N Engl J Med* 2020; **383:** 120–28.

3 Zeng J-H, Liu Y-X, Yuan J, et al. First case of COVID-19 complicated with fulminant myocarditis: a case report and insights. *Infection* 2020; published online April 10. https://doi.org/10.1007/s15010-020-01424-5.

4 Lax SF, Skok K, Zechner P, et al. Pulmonary arterial thrombosis in COVID-19 with fatal outcome: results from a prospective, single-center, clinicopathologic case series. *Ann Intern Med* 2020; **173:** 350–61.

5 Wichmann D, Sperhake J-P, Lütgehetmann M, et al. Autopsy findings and venous thromboembolism in patients with COVID-19: a prospective cohort study. *Ann Intern Med* 2020; **173:** 268–77.

6 Fox SE, Akmatbekov A, Harbert JL, Li G, Brown JQ, Vander Heide RS. Pulmonary and cardiac pathology in COVID-19: the first autopsy series from New Orleans. *medRxiv* 2020; published online April 10. https://doi.org/10.1101/2020.04.06.20050575 (preprint).

7 Fox SE, Akmatbekov A, Harbert JL, Li G, Quincy Brown J, Vander Heide RS. Pulmonary and cardiac pathology in African American patients with COVID-19: an autopsy series from New Orleans. *Lancet Respir Med* 2020; **8:** 681–86.

8 Carsana L, Sonzogni A, Nasr A, et al. Pulmonary post-mortem findings in a series of COVID-19 cases from northern Italy: a two-centre descriptive study. *Lancet Infect Dis* 2020; published online June 8. https://doi.org/10.1016/S1473-3099(20)30434-5.

9 Barton LM, Duval EJ, Stroberg E, Ghosh S, Mukhopadhyay S. COVID-19 autopsies, Oklahoma, USA. *Am J Clin Pathol* 2020; **153:** 725–33.

10 Puelles VG, Lütgehetmann M, Lindenmeyer MT, et al. Multiorgan and renal tropism of SARS-CoV-2. *N Engl J Med* 2020; **383:** 590–92.

11 Lamers MM, Beumer J, van der Vaart J, et al. SARS-CoV-2 productively infects human gut enterocytes. *Science* 2020; **369:** 50–54.

12 Tay MZ, Poh CM, Rénia L, MacAry PA, Ng LFP. The trinity of COVID-19: immunity, inflammation and intervention. *Nat Rev Immunol* 2020; **20:** 363–74.

13 Fang Y, Pekosz A, Haynes L, Nelson EA, Rowland RRR. Production and characterisation of monoclonal antibodies against the nucleocapsid protein of SARS-CoV. In: Perlman S, Holmes KV (eds). The nidoviruses. Advances in experimental medicine and biology, volume 581. Boston, MA: Springer, 2006: 153–56.

14 Rockx B, Kuiken T, Herfst S, et al. Comparative pathogenesis of COVID-19, MERS, and SARS in a nonhuman primate model. *Science* 2020; **368:** 1012–15.

15 International Society of Nephrology. KDIGO clinical practice guideline for acute kidney injury. Reference keys. *Kidney Int Suppl* 2012; **2:** 4.

16 van der Linden A, Blokker BM, Kap M, Weustink AC, Riegman PHJ, Oosterhuis JW. Post-mortem tissue biopsies obtained at minimally invasive autopsy: an RNA-quality analysis. *PLoS One* 2014; **9:** e115675.

17 Koppelkamm A, Vennemann B, Lutz-Bonengel S, Fracasso T, Vennemann M. RNA integrity in post-mortem samples: influencing parameters and implications on RT-qPCR assays. *Int J Legal Med* 2011; **125:** 573–80.

18 Nunes Duarte-Neto A, de Almeida Monteiro RA, da Silva LFF, et al. Pulmonary and systemic involvement of COVID-19 assessed by ultrasound-guided minimally invasive autopsy. *Histopathology* 2020; **77:** 186–97.

19 Schaller T, Hirschbühl K, Burkhardt K, et al. Postmortem examination of patients with COVID-19. *JAMA* 2020; **323:** 2518–20.

20 Tian S, Hu W, Niu L, Liu H, Xu H, Xiao SY. Pulmonary pathology of early-phase 2019 novel coronavirus (COVID-19) pneumonia in two patients with lung cancer. *J Thorac Oncol* 2020; **15:** 700–04.

21 Liu J, Zheng X, Tong Q, et al. Overlapping and discrete aspects of the pathology and pathogenesis of the emerging human pathogenic coronaviruses SARS-CoV, MERS-CoV, and 2019-nCoV. *J Med Virol* 2020; **92:** 491–94.

22 van den Brand JMA, Haagmans BL, van Riel D, Osterhaus ADME, Kuiken T. The pathology and pathogenesis of experimental severe acute respiratory syndrome and influenza in animal models. *J Comp Pathol* 2014; **151:** 83–112.

23 Nakajima N, Sato Y, Katano H, et al. Histopathological and immunohistochemical findings of 20 autopsy cases with 2009 H1N1 virus infection. *Mod Pathol* 2012; **25:** 1–13.

24 Su H, Yang M, Wan C, et al. Renal histopathological analysis of 26 postmortem findings of patients with COVID-19 in China. *Kidney Int* 2020; **98:** 219–27.

25 Michaud K, Basso C, d'Amati G, et al. Diagnosis of myocardial infarction at autopsy: AECVP reappraisal in the light of the current clinical classification. *Virchows Arch* 2020; **476:** 179–94.

26 Lindner D, Fitzek A, Bräuninger H, et al. Association of cardiac infection with SARS-CoV-2 in confirmed COVID-19 autopsy cases. *JAMA Cardiol* 2020; published online July 27. https://doi.org/10.1001/jamacardio.2020.3551.

27 von Weyhern CH, Kaufmann I, Neff F, Kremer M. Early evidence of pronounced brain involvement in fatal COVID-19 outcomes. *Lancet* 2020; **395:** e109.

28 Varga Z, Flammer AJ, Steiger P, et al. Endothelial cell infection and endotheliitis in COVID-19. *Lancet* 2020; **395:** 1417–18.

29 Puntmann VO, Carerj ML, Wieters I, et al. Outcomes of cardiovascular magnetic resonance imaging in patients recently recovered from coronavirus disease 2019 (COVID-19). *JAMA Cardiol* 2020; published online July 27. https://doi.org/10.1001/jamacardio.2020.3557.

30 Solomon IH, Normandin E, Bhattacharyya S, et al. Neuropathological features of COVID-19. *N Engl J Med* 2020; **383:** 989–92.

31 Vaira LA, Salzano G, Deiana G, De Riu G. Anosmia and ageusia: common findings in COVID-19 patients. *Laryngoscope* 2020; **130:** 28692.

32 Chamberlin NL. Functional organization of the parabrachial complex and intertrigeminal region in the control of breathing. *Respir Physiol Neurobiol* 2004; **143:** 115–25.

33 Schönrich G, Raftery MJ. Neutrophil extracellular traps go viral. *Front Immunol* 2016; **7:** 366.

34 Fuchs TA, Brill A, Duerschmied D, et al. Extracellular DNA traps promote thrombosis. *Proc Natl Acad Sci USA* 2010; **107:** 15880–85.

35 Jansen MPB, Emal D, Teske GJD, Dessing MC, Florquin S, Roelofs JJTH. Release of extracellular DNA influences renal ischemia reperfusion injury by platelet activation and formation of neutrophil extracellular traps. *Kidney Int* 2017; **91:** 352–64.

36 Brandes M, Klauschen F, Kuchen S, Germain RN. A systems analysis identifies a feedforward inflammatory circuit leading to lethal influenza infection. *Cell* 2013; **154:** 197–212.

37 Tang BM, Shojaei M, Teoh S, et al. Neutrophils-related host factors associated with severe disease and fatality in patients with influenza infection. *Nat Commun* 2019; **10:** 3422.

38 Barnes BJ, Adrover JM, Baxter-Stoltzfus A, et al. Targeting potential drivers of COVID-19: neutrophil extracellular traps. *J Exp Med* 2020; **217:** 1–7.

39 The RECOVERY Collaborative Group. Dexamethasone in hospitalized patients with Covid-19—preliminary report. *N Engl J Med* 2020; published online July 17. https://doi.org/10.1056/NEJMoa2021436.